Calibration of terahertz sampling detectors for intense unipolar picosecond current pulses in waveguides

Eva Díaz, Alberto Anadón, Martina Morassi, Michel Hehn, Aristide Lemaître, Jon Gorchon

Calibration of terahertz sampling detectors for intense unipolar picosecond current pulses in waveguides

Eva Díaz[1], Alberto Anadón[1], Martina Morassi[2], Michel Hehn[1], Aristide Lemaître[2], Jon Gorchon[1,*]

[1]Université de Lorraine, CNRS, IJL, F-54000 Nancy, France
[2]Université Paris-Saclay, CNRS, Centre de Nanosciences et de Nanotechnologies, 91120, Palaiseau, France
*e-mail: jon.gorchon@univ-lorraine.fr

Terahertz pulses are nowadays commonly used in many areas of condensed matter physics to access material properties and explore transport phenomena at fast timescales. However, little work has been devoted to the full characterization of such pulses when confined in waveguides. In this work we fabricate terahertz photoconductive switch detectors, located at various points along a coplanar waveguide, and sample the electrical pulses that pass by the detectors. Two different but consistent methods were developed to calibrate the pulse amplitude. Notably, we synchronize a commercial pulse generator with the laser in order to sample nanosecond-wide pulses with the photoswitch detectors, effectively turning the setup into an on-chip high-frequency sampling oscilloscope. Both methods give identical results on pulse current, voltage and field amplitudes and enable an absolute characterization of the electrical pulse propagation along the waveguide. These techniques constitute a reliable tool to explore (non-linear) phenomena such as current or field induced magnetization switching or phase transitions, which take place at high THz intensities.

The terahertz (THz) band, from ~ 100 GHz to ~10 THz, has been historically a difficult area of the spectrum to access due to the scarcity of sources, detectors and components in this range. Nowadays though, enough solutions exist so that the interest on the use of THz has raised in many fields. Notably, the field of spintronics, conventionally limited to the sub-GHz, GHz and optical regimes for a long time, is now overtaken by THz studies where unexpected dynamics[1–5] and resonant modes have been observed[6–8]. Some of these works, particularly when dealing with magnetization manipulation, require high fluence THz pulses, preferably of unipolar character. For this purpose, Auston photoconductive-switches are ideal sources[9–12]. In such switches, a femtosecond laser pulse is used to close transiently the switch, releasing part of the energy capacitively stored. The resulting picosecond electrical pulse can be then guided and focused down via tapered waveguides. However, since their inception in the 1980's, only a few works have discussed methods to characterize the picosecond pulse amplitude propagating into the waveguides[13–20]. Most methods are based on an electro-optic crystal[13–16], which has to be carefully positioned on the waveguide. This crystal can however potentially affect the propagating pulse[21]. Another interesting alternative is electro-absorption[17,18], but this method requires either multi-wavelength experiments[17] or layer-transfer techniques[18] which further complicates the fabrication process and/or experiments. Finally, the most common technique to characterize on-chip picosecond pulses consists in using photoswitches as detectors[9,10,22]. However, only few works have actually succeeded in calibrating accurately the signal amplitude[19,20]. Furthermore, these works have only focused on coplanar stripline designs and low voltages up to a few hundreds of mV[19,20]. Whether these calibrations remain valid at high bias voltages is still unknown[10101010]. Moreover, in many cases coplanar striplines might not be of interest, such as when dealing with an impedance matched termination that shorts both of the lines together and makes the photo-switch biasing impossible.

In this work we fabricated coplanar waveguides (CPW) incorporating picosecond pulse generating photoswitches, as well as photoswitch-based on-chip detectors. The detectors are almost transparent to the electrical pulses, but still highly sensitive. We calibrate the generated pulse amplitude via two distinct methods over several decades of powers up to the waveguide failure, and reach voltages, currents and fields of 20 V, 0.4 A and ~ 40 kV/cm respectively. In the process, we were able to synchronize nanosecond pulses from an external source with the laser, and detect the transient electric fields generated in the waveguides with high temporal resolution. This calibration method enables a complete characterization of picosecond-wide electrical pulses in waveguides including their propagation properties, bandwidth, intensity and the power delivered to an arbitrary load.

Our photoswitches use a low-temperature grown GaAs substrate (LT-GaAs). The substrate was fabricated by molecular beam epitaxy (MBE) in three steps: first, a dual buffer layer consisting of 400 nm of high-temperature GaAs followed by 300 nm of $Al_{0.33}GaAs_{0.67}$ is grown on a semi-conducting GaAs (100) substrate. The AlGaAs layer insulates electrically the LT-GaAs layer from the buffer. Secondly, a 1 µm thick layer of LT-GaAs is deposited at 260°C. This is the photo-active layer. Lastly, we annealed the sample in-situ at 600°C under an As atmosphere to

increase its resistivity[23]. The annealing contributes to reducing the number of defects in the LT-GaAs and thus to decreasing the number of conduction states in the semiconducting gap[23]. This way, the dark-current leakage (non-illuminated) through the photoswitch remains below 40 nA even at high biases (~100 V), leading to a better energy build-up and subsequent discharges.

lithography step, a Ti(10 nm)/Au(300 nm) bilayer is deposited and patterned to define the CPW structure, including the photoswitches and a tapered section which increases the electric field and current densities at the DUT. With the taper, the high current densities or fields needed in experiments such as magnetization reversal can be attained[4]. The structures are

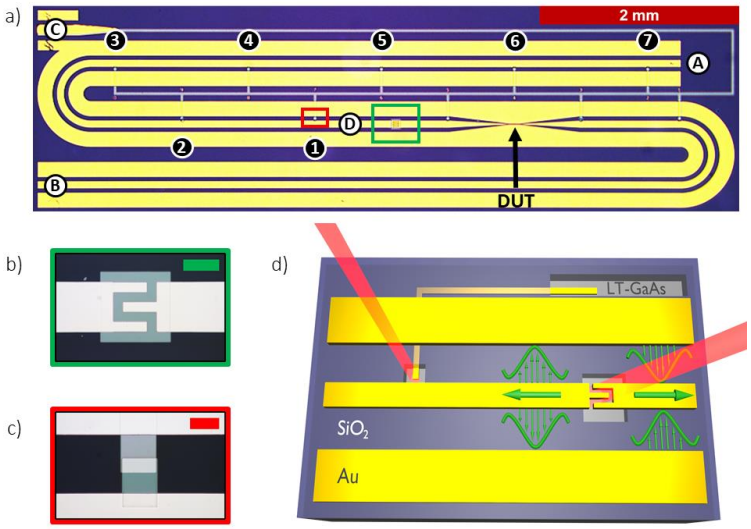

Fig. 1. Samples used for generation and detection of picosecond current pulses. a) Micrograph of the waveguide, including the b) emitter (scale bar: 50 µm) and c) detector photoconductive switches (scale bar: 20 µm), the latter identified from 1 to 7. The sample may also include a device under test (DUT). d) A pump laser beam excites the emitter on the right-side, which leads to a pair of current pulses propagating in opposite directions. The electric field, in between the conductors will accelerate the photo-generated charge due to the laser probe when reaching the detector's position on the left side. The read current is proportional to the pulse's amplitude.

Our devices consist of coplanar waveguides (Fig. 1.a) with an interdigitated *emitter* photo-switch (Fig. 1.b) embedded into the central transmission line. It generates intense picosecond electrical pulses. The waveguide includes various *detector* photo-switch arms (1 to 7 left of the emitter in Fig. 1.a, closeup in Fig. 1.c) that are located within the gap in-between the waveguide conductors to detect the transient electric fields induced by the propagating pulses, as in Auston et al.[9]. The waveguides have been lengthened into an S shape to increase the delay at which reflections from the ends would return (in the case of impedance mismatching), and avoid overlaps during pulse detection. The devices are fabricated by UV lithography and lift-off process in three steps (see structure schematic on Fig. 1.d). In the first step, a Ti(10 nm/)Au(20 nm)/Ti(3 nm) trilayer is deposited and patterned to form the detector arms. They all share the same potential, and are connected at position C. The Ti top layer, which gets slightly oxidized, serves as an adhesion layer for the following oxide layer. In the second step, a 100-nm layer of SiO_2 is deposited covering the totality of the surface, to avoid leaking currents through the substrate between metallic electrodes. Openings are patterned in the SiO_2 layer at the emitter and detector positions to define the photoswitches, as well as at position C, to ensure proper ohmic contacts. Finally, in the third

designed to have a 50 Ω impedance. Care was taken to insulate electrically the detector arm from the CPW. Additionally, before the last Au step, an extra step can be added to include a sample or device under test (DUT) to study with picosecond electrical pulses.

The photoconductive switches are activated by an amplified Ytterbium PHAROS® (Light Conversion) laser system, which generates ~250 fs-wide optical pulses at a center wavelength of 785 nm, via an optical parametric amplifier (ORPHEUS-F®). The repetition rate is tunable from 100 kHz down to on-demand single-shots. The beam is first divided into pump and probe beams via a beamsplitter. The pump goes through an optical delay line of ~13 ns and is focused on the generator photoswitch with a singlet lens with a ~40 µm FWHM spot size. The probe is focused down to ~25 µm onto the detector gap through a 2x objective.

To perform our calibration operations, we study pulses propagating towards the left of the emitter, away from the DUT. To this aim, two 20 GHz custom probes are connected at the ends of the CPW, on positions A and B. The switch is biased (V_{bias}) at position B with a Keithley 2400 source-meter and the waveguide

terminated at position A with an impedance-matched 50 Ω resistor, to minimize reflections. Next, the pump laser excitation gives rise to a pair of equal picosecond pulses (of opposite polarity) being generated and propagating towards the left and right (see Fig. 1.d), away from the emitter[9]. The photoswitch detection method[9] works as follows: by focusing the probe laser onto the detector arm 1 (see Fig. 1.a), the photoswitch is turned on transiently. As a result, a measurable current (I_{read}) flows into the detector proportional to the local electric field. The picosecond electrical pulse shape is resolved by changing the delay between the pump and the probe (see Fig. 2.a).

We use a double modulation of both the electrical pulse and the optical probe to achieve a reduction in the 1/f pink noise and leakage signals (such as the pump activating the detectors). Two modulation schemes were tested with success:

Scheme i). The pump is modulated by a mechanical chopper at 140 Hz and the probe beam at 40 kHz by a pair of polarizers and a 20 kHz photo-elastic modulator. The detection current therefore contains a 40 kHz signal with two satellite peaks at 40 ± 0.14 kHz which carry the doubly modulated signal of interest. The detection signal is fed into the current input of the first lock-in and detected at the second harmonic frequency (40 kHz), using a short time-constant (300 µs) and small filter (6 dB/oct) to avoid filtering out the satellites. The output is then fed into a second lock-in, mixed with the 140 Hz reference signal, and detected with a larger 300 ms time constant and 18 dB/oct filter to increase the signal-to-noise ratio.

Scheme ii). The bias voltage is modulated from 0 to V_{bias} at around 1.1 kHz, and the probe at 140 Hz via the chopper. The signals are then sent to the two same lock-in stages, with the same time constants and filters, but now the signal of interest is the satellite at 1.1 + 0.14 kHz. The bias modulation can be tuned to even higher modulation rates (~50 kHz), since the typical capacitances of the devices[4] are rather low (< 10^{-14} F).

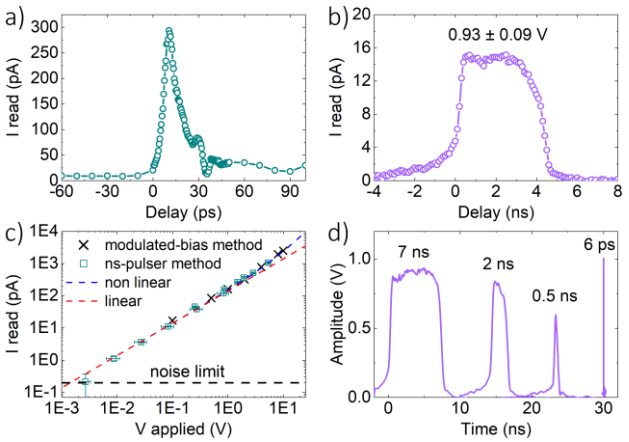

Fig. 2. a) A typical picosecond current pulse and b) 4 ns current pulse sampled by detector 1. c) The measured current as a function of the applied voltage to the detector, either statically (modulated bias method) or as pulses (nanosecond-pulser method). Both methods give the same linear response. d) A few examples of pulses of variable amplitude detected by detector 1 ranging from 7 ns to 6 ps.

To calibrate the detected signals, two different approaches are employed with comparable outcomes, giving high confidence in the measurements. In both cases the emitter photoswitch is not photo-excited, and a known electric field is applied to the waveguide instead.

The first and most straightforward method, consists in applying a *modulated bias* voltage at position A (see Fig. 1.a). The generated electric field then drives a current (I_{read}) into detector arm 1 independent of the delay time. This method has previously been used[19] for low voltages and a single modulation scheme, which may be prone to signal contamination. When using scheme i), the bias is modulated at 140 Hz, just as the pump was, while the PEM modulates the probe at 40 kHz. When using scheme ii), the bias is modulated at 1.1 kHz, and the probe is chopped at 140 Hz. This *modulated bias* approach is rather simple to implement but requires the center and ground lines to be opened on the detector side. If, however, the waveguide is terminated, for example with an impedance matched load, the method fails because no bias can be applied.

A second more universal approach is to synchronize the laser with an external electrical nanosecond (ns) pulser, and to sample ns pulses of known amplitude. To that end, the RF tip is repositioned from position B to position D, bypassing the photoswitch. The ns pulses are thus injected into the waveguide, sampled by detector 1 (see Fig. 2.b) and absorbed by the 50 Ω resistor on position A. To synchronize the ns pulses with the laser the optical pump beam is focused onto a fast Si photodiode, which then triggers an electronic delay generator with picosecond resolution. The delay generator then triggers the pulse generator. The delay can be varied either electronically or by the optical delay line. The

generated pulses are monitored with an oscilloscope before and after the waveguide, which gives the amplitude uncertainty (see legend in Fig. 2.b). This method could be further enhanced by fully characterizing the reflection and transmission coefficients of the waveguide and connections, for example with a vector network analyzer up to a few GHz.

This second *nanosecond-pulser* method, while having a larger uncertainty on the absolute voltage value in the waveguide, has the benefit of enabling direct comparison of pulses of various duration, from DC to picoseconds. The method is also universally compatible with any kind of waveguide as long as we can impedance match the external source to the waveguide or fully characterize the transmission and reflection coefficients of the system.

We compare both calibration methods in Fig. 2.c. and find the same *almost* linear relationship between the measured current (I_{read}) and the applied voltage over most of the range (see red fit). However, at high voltages, above the 100 mV explored by Kim et al.[19], a small non-linearity starts to take over (see blue fit). In fact, we can fit this non-linearity with a second-order correction term, proportional to V^2. Even though we do not have a proper understanding of the origin of such non-linearity at the moment, a proper characterization of this regime enables us to calibrate any high intensity pulses. Ultimately, in Fig. 2.d we show the potential of the technique to sample a wide range of electrical pulses, from the picosecond to nanosecond pulses (or longer). The amplitudes are all given in absolute values.

We note that scheme i) appears to suffer from aliasing due to the low laser repetition rate compared to the modulation frequency. However, in practice, by increasing the integration time, high signal-to-noise ratio can still be achieved. These signals, once calibrated, are consistent with results obtained through scheme ii).

These method's time resolution (and sensitivity bandwidth, see inset in Fig. 3.a) depends mostly on two factors. First, the detector photoswitch response function. If we assume that the detector response is similar to the emitter response, and that both processes can be described with Gaussians, then the deconvoluted current pulse duration should be $1/\sqrt{2}$ of the measured width. The second limiting factor is the synchronization between the electrical pulse generation and the optical probe. For photoswitch generated pulses this is not an issue since pump and probe beams are perfectly in sync as they are sourced from the same laser. However, when going through an electronic delay generator the jitter can be quite large. In the current experiments, we estimate the current jitter to be ~160 ps due to noise in the delay generator triggering. The jitter can be reduced down to the single picosecond level or lower, by either using a laser with active synchronization to an external clock or by feeding the laser clock into an electronic picosecond delay generator with ultralow jitter.

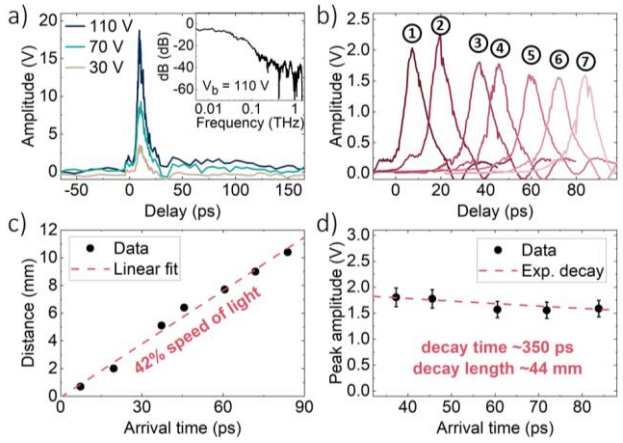

Fig. 3. a) Examples of picosecond-wide pulses characterized up to very high bias voltages (indicated in legend). The pulse-duration is not affected even at large biases. Inset: FFT of pulse generated at 110 V bias voltage. b) Pulses detected at different detectors. c) The distance of detectors from the emitter vs the arrival time of the pulses to each detector. The slope gives the phase velocity. d) The peak amplitude of the pulses as a function of their arrival time (to each detector) allows the extraction of decay times (and lengths).

When the detector is under a constant bias (as in the modulated bias calibration method), additional noise is picked up by the lock-in, increasing the calibration uncertainty. More importantly, measuring the pulse transient on the high voltage side of the photoswitch (where a discharge of the static voltage would take place) leads to noisier transients. This issue becomes particularly acute at high biases, probably due to much larger leakage currents and heating. Therefore, for clean and consistent results, the detector-side center-line is always kept connected to the ground, and the bias is applied on the other side of the photoswitch.

The calibration method described above for picosecond electrical pulses has been applied to three different photoswitch designs with different capacitances. As shown in Table 1, as expected, a larger capacitance implies a larger discharge but at the cost of a slightly increased pulse duration. The discharge is defined as the bias voltage fraction that effectively goes into the pulse. Both pulse duration and discharge remain more or less constant for increasing bias, with no observable pulse width and amplitude saturation even at biases above 100 V (see Fig. 3.a). We note that the emitter splits its energy into two equal and oppositely propagating pulses, which means only $V_{bias}/\sqrt{2}$ of the voltage is actually available for each pulse. The bias was increased until the waveguides failed. Remarkably, the photoswitches remained

intact at this point while the waveguide tapered section was destroyed due to the high current densities and the Joule heating in the highly lossy DUT region. Before failure, at the maximum discharge values, we were able to generate pulses of peak ~ 20 V, ~ 0.4 Amps and ~ 40 kV/cm at the tapered region. We postulate that by a) reducing the resistance (and absorption) of the DUT and/or b) using refractory metals, such as tungsten, for the waveguide tapered region, much larger electric fields and currents should be attainable without damage to the devices.

Switch	Capacitance (x 10^{-15} F)	Discharge (%) $= \sqrt{2} \cdot V_{peak}/V_{bias}$	FWHM (ps)
A	0.1	4.5 ± 0.1	8.7 ± 0.2
B	1.9	17 ± 1	9 ± 1
C	5.5	32.5 ± 0.3	11.6 ± 0.2

Table 1. Discharge percentage and pulse full width at half-maximum (FWHM) for 3 different emitter photoswitch designs (shown above). Capacitance is calculated as $C = \varepsilon_0 \varepsilon_r A/g$ where ε_0 is the vacuum permittivity, ε_r is the dielectric constant (13 for GaAs), A is the capacitor area, and g is the capacitor gap. Scale bar: 50 µm.

As shown in Fig. 2.d, our detection scheme has a minimum sensitivity of a few mV. We therefore cover a voltage detection range from a few mV up to tens of V. This kind of waveguide design could therefore be used in applications such as THz spectroscopy. In order to increase the sensitivity of the detectors, these can be placed closer to the center line, however this could result in larger reflections).

The pulse propagation can be characterized (see Fig. 3.b), by focusing the probe laser at several detector positions along the CPW (numbers 1-7 in Fig. 1.a). The phase velocity is extracted from the pulse arrival time at each detector which corresponds to 42% of the speed of light (shown in Fig. 3.c). Moreover, as shown in Fig. 3.d, the peak voltages can be fitted to an exponential decay, giving the decay time and length, found to be 350 ps and 44 mm, respectively (corresponding to -1 dB/4 mm). With a CPW total length around 20 mm, the pulse propagates through the entire CPW without significant dissipation. Note that the bend of the CPW between detectors 2 and 3 may induce a reflection and/or distortion of the transmitted pulse due a slight impedance mismatch. This could explain why the measurements performed at detectors 1 and 2 seem to follow a different trend than those made at detectors 3-7. Particularly, the larger signal on detector 2 might be attributed to a reflection from the bend (reflection should take about ~15ps to come back and could affect the readout). For this reason, the exponential decay is fitted with the next detectors' data (after the bend), as seen in Fig. 3.d. The implementation of a larger bend angle should resolve such issues.

In conclusion, we have implemented an on-chip photoconductive sampling device for electrical signal propagation sampling with picosecond resolution. We have developed two independent methods for amplitude calibration. With these methods, we characterize ps-wide pulses generated by a photoconductive switch embedded inside the CPW, and their propagation. The method sensitivity encompasses several decades in amplitude and power. This technique provides a simple and versatile tool for a variety of applications in the THz band.

Acknowledgments

E. D. would like to thank Dr. Junta Igarashi for his impedance-mismatched support, and Dr. Laurent Badie for his invaluable advice for sample fabrication. This work was supported by the ANR projects ANR-20-CE24-0003 SPOTZ and ANR-20-CE09-0013 UFO, by the impact project LUE-N4S part of the French PIA project "Lorraine Université d'Excellence", reference ANR-15IDEX-04-LUE, by the Région Grand Est and the Metropole Grand Nancy, for the Chaire PLUS and the "FEDER-FSE Lorraine et Massif Vosges 2014-2020", a European Union Program and by the French RENATECH network. This work was also partially supported by a government grant managed by the ANR as a part of the France 2030 investment plan from PEPR SPIN ANR-22-EXSP TOAST.

Competing financial interests

The authors declare no competing financial interests**.**

Data availability statement

The data that support the findings of this study are available from the corresponding author upon reasonable request.

References

[1] K. Neeraj, N. Awari, S. Kovalev, D. Polley, N. Zhou Hagström, S.S.P.K. Arekapudi, A. Semisalova, K. Lenz, B. Green, J. Deinert, I. Ilyakov, M. Chen, M. Bawatna, V. Scalera, M. D'Aquino, C. Serpico, O. Hellwig, J. Wegrowe, M. Gensch, and S. Bonetti, "Inertial spin dynamics in ferromagnets," Nat. Phys. **17**(2), 245–250 (2021).

[2] S. Schlauderer, C. Lange, S. Baierl, T. Ebnet, C.P. Schmid, D.C. Valovcin, A.K. Zvezdin, A.V. Kimel, R.V. Mikhaylovskiy, and R. Huber, "Temporal and spectral fingerprints of ultrafast all-coherent spin switching," Nature **569**(7756), 383–387 (2019).

[3] Y. Yang, R.B. Wilson, J. Gorchon, C.-H. Lambert, S. Salahuddin, and J. Bokor, "Ultrafast Magnetization Reversal by Picosecond Electrical Pulses," Sci. Adv., in press, arXiv: 1609.06392 (2017).

[4] K. Jhuria, J. Hohlfeld, A. Pattabi, E. Martin, A. Ygnacio, A. Córdova, X. Shi, R.L. Conte, S. Petit-watelot, J.C. Rojas-sanchez, G. Malinowski, S. Mangin, A. Lemaître, M. Hehn, J. Bokor, R.B. Wilson, and J. Gorchon, "Spin–orbit torque switching of a

ferromagnet with picosecond electrical pulses," Nat. Electron., (2020).
[5] S. Bonetti, M.C. Hoffmann, M.J. Sher, Z. Chen, S.H. Yang, M.G. Samant, S.S.P. Parkin, and H.A. Dürr, "THz-Driven Ultrafast Spin-Lattice Scattering in Amorphous Metallic Ferromagnets," Phys. Rev. Lett. **117**(8), 1–5 (2016).
[6] T. Kampfrath, A. Sell, G. Klatt, A. Pashkin, S. Mährlein, T. Dekorsy, M. Wolf, M. Fiebig, A. Leitenstorfer, and R. Huber, "Coherent terahertz control of antiferromagnetic spin waves," Nat. Photonics **5**(1), 31–34 (2011).
[7] P. Vaidya, S.A. Morley, J. Van Tol, Y. Liu, R. Cheng, A. Brataas, D. Lederman, and E. Del Barco, "Subterahertz spin pumping from an insulating antiferromagnet," Science, **368**(6487), 160–165 (2020).
[8] J. Li, C.B. Wilson, R. Cheng, M. Lohmann, M. Kavand, W. Yuan, M. Aldosary, N. Agladze, P. Wei, M.S. Sherwin, and J. Shi, "Spin current from sub-terahertz-generated antiferromagnetic magnons," Nature **578**(7793), 70–74 (2020).
[9] D.H. Auston, A.M. Johnson, P.R. Smith, and J.C. Bean, "Picosecond optoelectronic detection, sampling, and correlation measurements in amorphous semiconductors," Appl. Phys. Lett. **37**(4), 371–373 (1980).
[10] D.H. Auston, in *Semicond. Semimet.* (Elsevier, 1990), pp. 85–134.
[11] R.A. Lewis, "A review of terahertz sources," (2014).
[12] J. Gorchon, M. Hehn, G. Malinowski, and S. Mangin, "Electronic transport induced ultrafast magnetization switching," J. Magn. Magn. Mater. **563**, 169919 (2022).
[13] T. Motet, J. Nees, S. Williamson, and G. Mourou, "1.4 ps rise-time high-voltage photoconductive switching," Appl. Phys. Lett. **59**(12), 1455–1457 (1991).
[14] H.M. Heiliger, M. Vossebürger, H.G. Roskos, R. Hey, K. Ploog, and H. Kurz, "THz Signal Generators Based on Lift-Off LT-GaAs on Transparent Substrates," Seventh Int. Symp. Space Terahertz Technol. **1**(March), 400 (1996).
[15] R. Adam, M. Mikulics, A. Förster, J. Schelten, M. Siegel, P. Kordoš, X. Zheng, S. Wu, and R. Sobolewski, "Fabrication and subpicosecond optical response of low-temperature-grown GaAs freestanding photoconductive devices," Appl. Phys. Lett. **81**(18), 3485–3487 (2002).
[16] X. Zheng, Y. Xu, R. Sobolewski, R. Adam, M. Mikulics, M. Siegel, and P. Kordos, "Femtosecond response of a free-standing LT-GaAs photoconductive switch.," Appl. Opt. **42**(9), 1726–31 (2003).
[17] J.F. Lampin, L. Desplanque, and F. Mollot, "Detection of picosecond electrical pulses using the intrinsic Franz–Keldysh effect," Appl. Phys. Lett. **78**(26), 4103–4105 (2001).
[18] L. Desplanque, J.F. Lampin, and F. Mollot, "Generation and detection of terahertz pulses using post-process bonding of low-temperature-grown GaAs and AlGaAs," Appl. Phys. Lett. **84**(12), 2049–2051 (2004).
[19] J. Kim, S. Williamson, J. Nees, S. Wakana, and J. Whitaker, "Photoconductive sampling probe with 2.3-ps temporal resolution and 4-μV sensitivity," Appl. Phys. Lett. **62**(18), 2268–2270 (1993).
[20] J. Hwang, R.K. Lai, J. Nees, T. Norris, and J.F. Whitaker, "A field-sensitive photoconductive probe for sampling through passivation layers," Appl. Phys. Lett. **69**(15), 2211–2213 (1996).
[21] R.A. Lewis, "A review of terahertz detectors," J. Phys. Appl. Phys. **52**(43), (2019).
[22] D.R. Grischkowsky, M.B. Ketchen, C.-C. Chi, I.N. Duling, N.J. Halas, J.-M. Halbout, and P.G. May, "Capacitance Free Generation and Detection of Subpicosecond Electrical Pulses on Coplanar Transmission Lines," IEEE J. Quantum Electron. **24**(2), 221–225 (1988).
[23] I.S. Gregory, C. Baker, W.R. Tribe, M.J. Evans, H.E. Beere, E.H. Linfield, A.G. Davies, and M. Missous, "High resistivity annealed low-temperature GaAs with 100 fs lifetimes," Appl. Phys. Lett. **83**(20), 4199–4201 (2003).